Preparation and Ethanol Sensing Properties of In2O3 Nanotubes

Article *in* Journal of Nanoscience and Nanotechnology · May 2014

DOI: 10.1166/jnn.2014.8035

8 authors, including:

Wei Li

992 PUBLICATIONS **17,041** CITATIONS

SEE PROFILE

Chao Li

63 PUBLICATIONS **1,098** CITATIONS

SEE PROFILE

Fengdong Qu

Chinese Academy of Sciences

41 PUBLICATIONS **513** CITATIONS

SEE PROFILE

Wenbin Guo

Jilin University

207 PUBLICATIONS **1,350** CITATIONS

SEE PROFILE

Article

Journal of
Nanoscience and Nanotechnology
Vol. 14, 3653–3657, 2014
www.aspbs.com/jnn

Preparation and Ethanol Sensing Properties of In_2O_3 Nanotubes

Juan Liu[1], Wei Li[1], Linghui Zhu[1], Chao Li[1], Fengdong Qu[1], Wenbin Guo[1,*], Caihui Feng[1], and Shengping Ruan[2,*]

[1] State Key Laboratory on Integrated Optoelectronics, Jilin University, Changchun 130012, China
[2] College of Electronic Science and Engineering, Jilin University, Changchun 130012, China

In this paper, In_2O_3 nanotubes were prepared by an electrospinning method combined with an oriented-contract calcinations scheme, and characterized by differential thermal and thermal gravimetric analyzer (DTA-TGA), X-ray diffraction (XRD), and scanning electron microscopy (SEM). Ethanol sensing properties of the as-prepared nanotubes were investigated. The results showed that the In_2O_3 nanotubes were obtained at a fast heating rate of 100 °C/min. Ethanol sensing properties indicated that the nanotubes exhibit a high response of 87.5 to 500 ppm ethanol, fast response (20 s) and recovery (18 s) rate at the optimal operating temperature of 260 °C. Moreover, the nanotubes also exhibit good selectivity.

Keywords: Electrospinning, In_2O_3 Nanotubes, Gas Sensor, Ethanol.

1. INTRODUCTION

Sensor technology is one of the most important key technologies of the future with a constantly increasing number of applications, both in the industrial and in the private sectors. More and more gas sensors are used for the control of technical processes, in environment monitoring, healthcare, and automobiles.[1] As an important branch of gas sensors, chemical sensors based on semiconductor metal oxide one dimensional (1D) nanomaterials (nanorod, nanofiber, nanowire, nanobelts, and nanotube etc.)[2] have been stimulated and facilitated by the convenience of a large number of available fabrication methods like template-assisted sol–gel, chemical vapor deposition (CVD), electrospinning, hydrothermal etc.[3–7] Among them, electrospinning emerged as a simple and versatile method for generating nanofibers nanobelts, and nanotubes with large surface area to volume ratios and porous structures[8–10] A large surface area can provide relatively mass reactive sites, while a porous structure can form relatively loose film structures which is an advantage for gas diffusion and beneficial for gas sensing.[11]

In_2O_3, an *n*-type semiconductor with a direct bandgap of 3.55–3.75 Ev,[12] has been widely applied in optoelectronic device such as UV lasers, gas sensors, solar cells, flat-panel displays, and so forth.[13–17] As for gas sensing applications, In_2O_3 with different morphologies have been prepared to detect ethanol, H_2S, NO_2, NH_3, CO, and H_2,[18–24] due to its low resistance, good catalysis, strong interaction with the poisonous gas molecules, high sensitivity and large number of detectable gases. In order to further improve gas sensing properties of In_2O_3, two methods are usually adopted: one is decorating In_2O_3 with noble metal (like Pt, Ag, Au, Pd) or metal oxide (CoO, CuO, NiO),[25–28] the other is increasing its surface area since gas sensing reaction is a surface-controlled process. Many researches focused on decreasing the nanoparticle size of In_2O_3, or developing solid In_2O_3 1D nanostructure to improve the surface areas of In_2O_3. The hollow In_2O_3 1D nanostructure, which have both inter- and outer-surfaces, are promising gas sensing materials and researched relatively little.

In this paper, In_2O_3 nanotubes were prepared by facile electrospinning method combined with an oriented-contract scheme. Their ethanol sensing properties were also investigated. Highly efficient ethanol sensing properties were observed, which makes the fabricated nanomaterial a good candidate for high performance ethanol sensors.

2. EXPERIMENTAL DETAILS

2.1. Chemical Reagent

All the starting materials (AR grade): $In(NO_3)_3 \cdot 4.5H_2O$, C_2H_5OH, *N*,*N*-dimethylformamide (DMF), and Polyvinyl

*Authors to whom correspondence should be addressed.

pyrrolidone (PVP, $M_w \approx 1{,}300{,}000$) were purchased from Aladdin Chemistry Co. Ltd.

2.2. Preparation of In_2O_3 Nanotubes

In a typical process, ethanol and *N*,*N*-dimethylformamide (DMF) were mixed together with a weight ratio of 1:1. Then, a certain amount of $In(NO_3)_3 \cdot 4.5H_2O$ were added into the above solvent. After stirring for 2 h, PVP was added to the above mixtures and continuously stirred for another 6 h. The obtained solution was then transferred into a plastic syringe with a metal needle, which was connected to a high-voltage power supply. A voltage of 20 kV was applied between the cathode (a flat aluminum foil) and the anode (syringe tip) at a distance of 20 cm. The $In(NO_3)_3$/PVP composite nanofibers were collected. The composite nanofibers were transferred into the muffle and then annealed at 600 °C for 2 h with a heating rate of 1 °C/min and 100 °C/min, respectively. After the fibers were naturally cooled to room temperature, the In_2O_3 nanofibers/nanotubes were obtained

2.3. Characterization

The nanotubes we prepared were characterized by differential thermal analyzer (DTA) and thermal gravimetric analyzer (TGA) (Melttler Toledo 825^e); X-ray diffractometer (XRD) (Shimadzu XRD-6000, Cu-Kα radiation); and scanning electron microscopy (SEM) (XL30 ESEMFEG).

2.4. Sensor Fabrication and Measurement

The gas sensor was fabricated as follows: the as-synthesized sample was mixed with deionized water in a weight ratio of 100:25 to form a paste. Then the paste was coated on Al_2O_3 substrates with Ag-Pd electrodes (finger spacing: 200 μm, finger depth: 20 μm, 13.4 mm in length, 7 mm in width) to form a sensing film. Finally the sensor was preheated at 300 °C for 24 h before measuring. The gas sensing properties of the sensor were measured by a CGS-1TP intelligent gas sensing analysis system (Beijing Elite Tech Co. Ltd., China).

The sensor response (S) was measured between 230 and 290 °C by comparing the resistance of the sensor in air (R_a) with that in target gases (R_g). The time taken by the sensor to achieve 90% of the total resistance change was defined as the response time in the case of adsorption or the recovery time in the case of desorption.

3. RESULTS AND DISCUSSION

3.1. Nanofiber Characterization

To find an appropriate calcination scheme, the Differential thermal and thermal gravimetric analysis was carried out and the results are shown in Figure 1. It is clear from the TGA curve that before 220 °C, the first stage of weight loss was about 6% which may be caused by the evaporation of volatiles (ethanol and H_2O). The second stage is

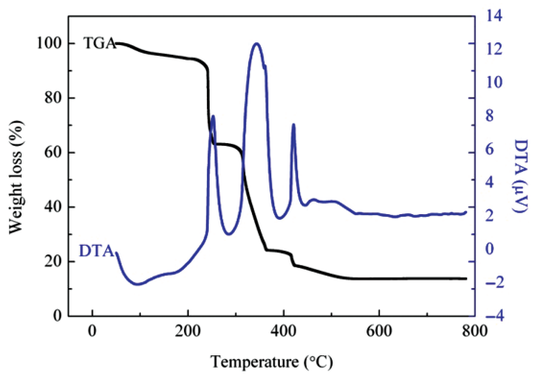

Figure 1. DTA-TGA curves of the $In(NO_3)_3$/PVP composite nanofibers.

from 220 °C to 413 °C with a weight loss about 64.2% and corresponds to two obvious exothermic peaks at 251.1 °C, 343.2 °C respectively. In this stage, $In(NO_3)_3$ and DMF were wholly decomposed, together with the occurrence of intermolecular cross-linking reaction,[29] and the degradation of the side chain of PVP. The last stage between 413 °C and 550 °C with a weight loss of 8%, which corresponded to an exothermic peak at 422 °C, may be the result of carbon oxidation and the decomposition of the intra of PVP.[30]

The micro-morphology of In_2O_3 nanostructures were investigated by scanning electron microscopy. As shown in Figure 2(a), the $In(NO_3)_3$/PVP composite nanofibers were collected as randomly oriented structures in the form of nonwoven mats because of the bending instability associated with the spinning jet. Each fiber is uniform and smooth in the cross section with an average diameter about 360 nm.[31] The precursor fibers were then heated to 600 °C at rates of 1 °C/min and 100 °C/min, respectively. As shown in Figures 2(b) and (c), the surface of the In_2O_3 nanofibers/nanotubes becomes bend and rough, which is due to the removal of PVP and crystallization of In_2O_3. The average diameter decreased to about 70 nm for In_2O_3 nanofibers, while for the In_2O_3 nanotubes, the outer diameter and wall thickness are about 200 nm and 65 nm, respectively.

The XRD pattern of the In_2O_3 nanotubes is shown in Figure 3. From the curve it can be easily found that all the diffraction peaks are well in agreement with the body-centered cubic indium oxide (JCPDS card no.06-0416).[32] And no other diffraction peaks corresponding to any impurities exist, which indicated the fabricated In_2O_3 nanotubes had a higher purity.

The formation mechanism of In_2O_3 nanotubes can be explained as follows: as soon as the $In(NO_3)_3$/PVP composite nanofibers were obtained, a calcination process was followed. In this step, proper heating rate (R) is essential. The large temperature gradient along the radial direction can result in a dense rigid shell outside of the viscoelastic gel firstly. The outer shell and the inner gel will provide

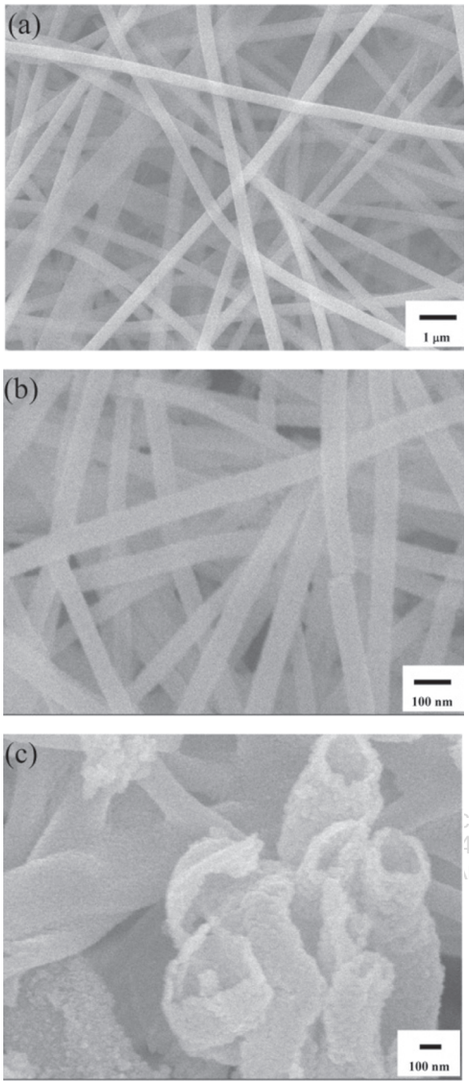

Figure 2. SEM images of the $In(NO_3)_3$/PVP composite nanofibers (a), In_2O_3 nanofibers (b), In_2O_3 nanotubes (c).

an adhesive force and a cohesive force to the interface layer between them respectively at the same time. And the direction of two forces is opposite. If the cohesive force is smaller than the adhesive force, the contraction of interface layer caused by the decomposition of organic and inorganic components will be towards the rigid shell. The nanotubes are then obtained correspondingly.[28]

3.2. Evaluation of Gas-Sensing Performance

The responses of In_2O_3 nanofibers/nanotubes to 500 ppm ethanol versus the operating temperature are displayed in Figure 4. As shown in Figure 4, the responses of the nanofibers/nanotubes to ethanol increased with the augment of operating temperatures that attained maximum values at 260 °C, finally decreased with further increasing of operating temperature.[33] The temperature 260 °C was

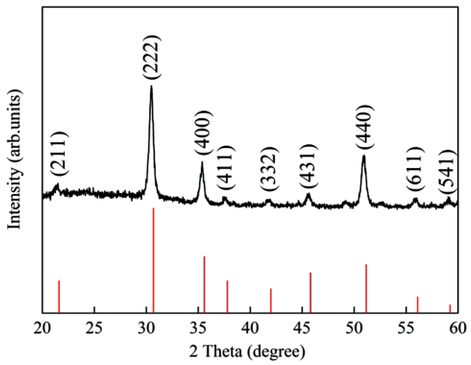

Figure 3. XRD pattern of the In_2O_3 nanotubes.

correspondingly identified as the optimum operating temperature and applied in all the investigations hereinafter. Moreover, in the whole temperature range, the In_2O_3 nanotubes exhibit much higher response than the In_2O_3 nanofibers. This may be attributed that the porous structure of In_2O_3 nanotubes can provide more reaction sites for both oxygen species and ethanol molecule compared with In_2O_3 nanofibers which is beneficial for the gas sening reaction.

As for gas sensing applications, rapid response and recovery are of great importance. Figure 5 shows the response and recovery characteristic of the In_2O_3 nanotubes to 500 ppm ethanol at 260 °C. It can be seen that when the target gas was injected into the testing chamber, the responses of the sensors increase rapidly; when subjected to air the sensor recovery to the initial state was also rapid. The response time is about 20 s while the recovery time is about 18 s. The rapid response and recovery of the sensor can be attributed to the 1D nanostructure of our electrospun nanotubes, which can facilitate fast mass transfer of ethanol molecules to and from the interaction region as well as improve the rate for charge carriers to traverse the barriers introduced by molecular recognition events along the entire fibers.[34] Besides, the porous structure of

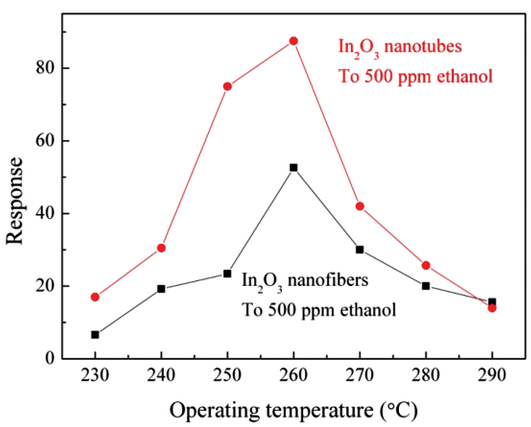

Figure 4. Responses of the In_2O_3 nanofibers/nanotubes versus operating temperature.

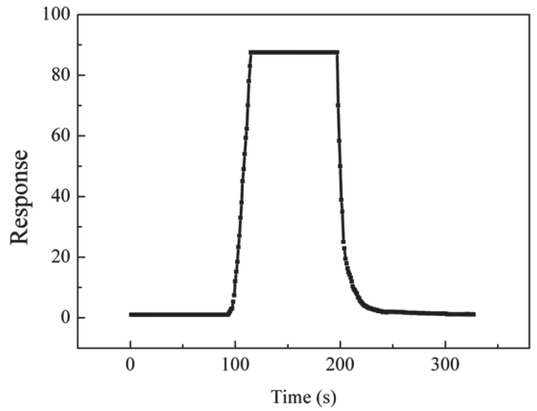

Figure 5. Response and recovery properties of the In_2O_3 nanotubes to 500 ppm ethanol at 260 °C.

the In_2O_3 nanotubes is also beneficial for fast response and recovery rate.

The gas sensing selectivity is another important parameter to evaluate the sensing ability of semiconductor materials. The cross-responses of In_2O_3 nanotubes to 500 ppm H_2, NO_2, C_8H_{10}, CO, CH_4, and HCHO at 260 °C are shown in the Figure 6. It can be seen that the response to ethanol is much larger than that to others which can be explained from the kinetics and mechanics of gas adsorption and desorption on the surface of In_2O_3 or similar semiconducting oxides.[35]

The sensing mechanism can be explained as follows. The response of semi-conducting metal oxides is based on the reactions between gas molecule to be detected and the oxygen species on the surface of oxides. When In_2O_3 nanotubes are surrounded by air, oxygen molecules can be absorbed on their surface to generate chemisorbed oxygen species,[36] which can lead to a decrease of tube conductive. When the sensor is exposed to ethanol, ethanol molecules can react with the chemisorbed oxygen species and release the trapped electron back to the conduction band, which will increase the carrier concentration and electron mobility and result in the reducing of fiber resistance. The high sensitivity of the current nanotubes are related to their 1D nanostructure which can make the sensor absorb more ethanol molecules, and can also form web-like structure on sensor surface naturally. Simultaneously, the porous structure of the In_2O_3 nanotubes can provide more adsorption sites, leading more oxygen species and ethanol molecules absorbed on the surface of In_2O_3 nanotubes, which eventually improve the sensing performances of In_2O_3 nanotubes. The observed high sensitivity and selectivity, fast response and recovery rate of the In_2O_3 nanotubes make the developed material suitable candidate for ethanol sensing.

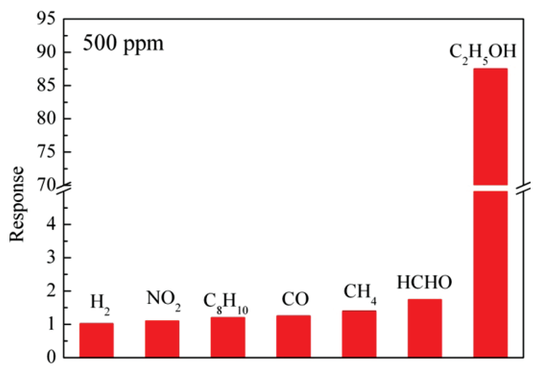

Figure 6. Cross-responses of In_2O_3 nanotubes to 500 ppm different gases at 260 °C.

4. CONCLUSIONS

In this paper, In_2O_3 nanotubes were prepared by an electrospinning method. Their ethanol sensing properties were also investigated. The results showed that compared with In_2O_3 nanofibers the porous structures of In_2O_3 nanotubes greatly improved their ethanol sensing properties. The sensor exhibits a high response of 87.5 to 500 ppm ethanol at the optimal operating temperature of 260 °C. Moreover, the sensor also exhibit fast response and recovery rate and good selectivity.

Acknowledgment: The authors are grateful to National Natural Science Foundation of China (Grant nos. 61006013, 61007022, 61275035, 61274068, 61077046), Chinese National Programs for High Technology Research and Development (Grant nos. 2013AA030902), Doctoral Found of Ministry of Education of China (Grant nos. 20100061120045, 20110061130004), Project of Science and Technology Development Plan of Jilin Province (Grant nos. 20110314, 20120324), the Opened Fund of the State Key Laboratory on Integrated Optoelectronics (No. IOSKL2012KF03) for the support to the work.

References and Notes

1. M. E. Franke, T. J. Koplin, and U. Simon, *Small* 2, 36 (**2006**).
2. K.-S. Lin and S. Chowdhury, *International Journal of Molecular Sciences* 11, 3226 (**2010**).
3. B. B. Lakshmi, P. K. Dorhout, and C. R. Martin, *Chem. Mater.* 9, 857 (**1997**).
4. G. Che, B. B. Lakshmi, C. R. Martin, E. R. Fisher, and R. S. Ruoff, *Chem. Mater.* 10, 260 (**1998**).
5. B. Ding, M. Wang, X. Wang, J. Yu, and G. Sun, *Mater. Today* 13, 16 (**2010**).
6. W. N. Li, J. Yuan, X. F. Shen, S. Gomez-Mower, L. P. Xu, S. Sithambaram, M. Aindow, and S. L. Suib, *Adv. Funct. Mater.* 16, 1247 (**2006**).
7. M. Batory, D. Batory, J. Grabarczyk, W. Kaczorowski, B. Kupcewicz, K. Mitura, T. H. Nasti, N. Yusuf, and P. Niedzielski, *J. Nanosci. Nanotechnol.* 12, 9037 (**2012**).
8. H. Jiang, Y. Hu, Y. Li, P. Zhao, K. Zhu, and W. Chen, *J. Controlled Release* 108, 237 (**2005**).
9. A. Yang, X. Tao, G. K. H. Pang, and K. G. G. Siu, *J. Am. Ceram. Soc.* 91, 257 (**2008**).
10. D. Li, J. T. McCann, Y. Xia, and M. Marquez, *J. Am. Ceram. Soc.* 89, 1861 (**2006**).
11. Y.-F. Sun, S.-B. Liu, F.-L. Meng, J.-Y. Liu, Z. Jin, L.-T. Kong, and J.-H. Liu, *Sensors* 12, 2610 (**2012**).

12. C. Feng, W. Li, C. Li, L. Zhu, H. Zhang, Y. Zhang, S. Ruan, W. Chen, and L. Yu, *Sensors and Actuators B: Chemical* 166, 83 **(2012)**.
13. H. Imai, A. Tominaga, H. Hirashima, M. Toki, and M. Aizawa, *Journal of Sol–Gel Science and Technology* 13, 991 **(1998)**.
14. E. Comini, A. Cristalli, G. Faglia, and G. Sberveglieri, *Sensors and Actuators B: Chemical* 65, 260 **(2000)**.
15. Y. Ogawa, A. Jäger-Waldau, Y. Hashimoto, and K. Ito, *Japanese Journal of Applied Physics* 33, L1775 **(1994)**.
16. R. G. Gordon, *MRS Bull.* 25, 52 **(2000)**.
17. K. Kato, H. Omoto, and M. Yonekura, *J. Nanosci. Nanotechnol.* 12, 9183 **(2012)**.
18. K. K. Makhija, A. Ray, R. M. Patel, U. B. Trivedi, and H. N. Kapse, *Bull. Mater. Sci.* 28, 9 **(2005)**.
19. Z. Zeng, K. Wang, Z. Zhang, J. Chen, and W. Zhou, *Nanotechnology* 20, 045503 **(2009)**.
20. D. Zhang, Z. Liu, C. Li, T. Tang, X. Liu, S. Han, B. Lei, and C. Zhou, *Nano Letters* 4, 1919 **(2004)**.
21. N. Du, H. Zhang, B. D. Chen, X. Y. Ma, Z. H. Liu, J. B. Wu, and D. R. Yang, *Adv. Mater.* 19, 1641 **(2007)**.
22. H. Yamaura, K. Moriya, N. Miura, and N. Yamazoe, *Sensors and Actuators B: Chemical* 65, 39 **(2000)**.
23. S. Shukla, S. Seal, L. Ludwig, and C. Parish, *Sensors and Actuators B: Chemical* 97, 256 **(2004)**.
24. B. Chamnankid, R. Samanpratan, and P. Kongkachuichay, *J. Nanosci. Nanotechnol.* 12, 9325 **(2012)**.
25. C. A. Papadopoulos, D. S. Vlachos, and J. N. Avaritsiotis, *Sensors and Actuators B: Chemical* 32, 61 **(1996)**.
26. Y. Zhang, Z. Zheng, and F. Yang, *Ind. Eng. Chem. Res.* 49, 3539 **(2010)**.
27. C.-Y. Liu, T. Hasty, and A. J. Bard, *J. Electrochem. Soc.* 143, 1914 **(1996)**.
28. J. T. McCue and J. Y. Ying, *Chem. Mater.* 19, 1009 **(2007)**.
29. F. Mou, J.-G. Guan, W. Shi, Z. Sun, and S. Wang, *Langmuir* 26, 15580 **(2010)**.
30. Y. Zhang, J. Li, Q. Li, L. Zhu, X. Liu, X. Zhong, J. Meng, and X. Cao, *Scripta Mater.* 56, 409 **(2007)**.
31. I.-D. Kim, A. Rothschild, B. H. Lee, D. Y. Kim, S. M. Jo, and H. L. Tuller, *Nano Letters* 6, 2009 **(2006)**.
32. C. H. Liang, G. W. Meng, Y. Lei, F. Phillipp, and L. D. Zhang, *Adv. Mater.* 13, 1330 **(2001)**.
33. N. S. Ramgir, I. S. Mulla, and K. P. Vijayamohanan, *Sensors and Actuators B: Chemical* 107, 708 **(2005)**.
34. W. Wang, H. Huang, Z. Li, H. Zhang, Y. Wang, W. Zheng, and C. Wang, *J. Am. Ceram. Soc.* 91, 3817 **(2008)**.
35. Q. Qi, T. Zhang, L. Liu, X. Zheng, Q. Yu, Y. Zeng, and H. Yang, *Sensors and Actuators B: Chemical* 134, 166 **(2008)**.
36. W. Zheng, X. Lu, W. Wang, Z. Li, H. Zhang, Y. Wang, Z. Wang, and C. Wang, *Sensors and Actuators B: Chemical* 142, 61 **(2009)**.

Received: 1 September 2012. Accepted: 2 January 2013.